8B.3 Comparison of Observations of the Spatial Distribution of Water Vapor Derived from Radar and Radiometer Measurements during the DYNAMO Field Campaign

Swaroop Sahoo[1]*, Xavier Bosch-Lluis[1], Steven C. Reising[1],
J. Vivekanandan[2], Paquita Zuidema[3] and Scott M. Ellis[2]

[1] Microwave Systems Laboratory, Colorado State University, Fort Collins, CO 80523
[2] National Center for Atmospheric Research, Boulder, CO 80301
[3] Rosenstiel School of Marine and Atmospheric Science, University of Miami, Miami, FL 33149

ABSTRACT

The Dynamics of the Madden-Julian Oscillation (DYNAMO) field campaign was designed primarily to study the Madden-Julian oscillation (MJO) effect so that it can be understood and modeled. DYNAMO was designed to study important atmospheric parameters including vertical moisture profiles, cloud structure, precipitation processes and the planetary boundary layer. A variety of in-situ and remote sensing instruments were deployed during the campaign, including the S-PolKa radar by the National Center for Atmospheric Research (NCAR) and a collocated microwave radiometer (operating at 23.8 and 30.0 GHz) by the University of Miami. These instruments sampled common volumes of the atmosphere. This experimental configuration provided an opportunity to estimate slant water vapor during clear sky and cloudy conditions. These two instruments can be used to compare the amount of water vapor and liquid water present in the atmosphere at various azimuth and elevation angles. The goal of this study is to develop a retrieval algorithm for water vapor using radiometer measurements during clear sky conditions.

1. INTRODUCTION

The field campaign of Dynamics of the Madden-Julian Oscillation (DYNAMO) took place in the central equatorial Indian Ocean between September 1, 2011 and January 5, 2012. The experiment was primarily designed to improve understanding of the Madden-Julian oscillation (MJO) in that region. Observations of vertical moisture profiles, cloud structure, precipitation processes and the planetary boundary layer are necessary to improve understanding of MJO initiation. A number of remote sensing instruments, including the National Center for Atmospheric Research (NCAR)'s S-PolKa (dual-wavelength S- and Ka-band) radar [1] and the University of Miami's microwave radiometer, were deployed to estimate water vapor, liquid water and cloud structure.

This work focuses on retrieval of slant water path (SWP) from measurements by the K- and Ka-band radiometer at various elevation and azimuth angles during DYNAMO. Radiometric measurements were performed at 23.8 GHz, which is affected mostly by water vapor and will be used for SWP retrieval, and at 30.0 GHz, which is primarily sensitive to cloud liquid water [2] and will be used for estimating liquid water. Due to the low elevation angles at which the radiometric measurements were performed, the consistency and accuracy of the data has been studied to separate the effect of any land contamination from actual meteorological effects in which the azimuth dependence of brightness temperature may reflect water vapor and liquid water convergence induced by the diurnal heating of the atoll. Brightness temperatures at these two frequencies exhibit a linear relationship to SWP during clear sky conditions.

This work is organized into the following sections: Section 2 discusses the experiment setup for DYNAMO, while the measurements have been analyzed in Section 3 for detection of land contamination or any other anomalous behavior. The classification of the data into clear sky and cloudy sky conditions using the cloudy sky ratio has been developed and explained in detail in Section 4. Finally the summary and the future work are presented and discussed in Section 5.

2. EXPERIMENT DESCRIPTION

As part of the DYNAMO campaign the S-PolKa (dual-wavelength S and Ka-band) radar was deployed by NCAR and a two channel microwave radiometer was deployed by the University of Miami (known as UM-Radiometer in this paper) on Gan Island, The Maldives in the Indian Ocean. Another microwave radiometer was deployed by the U.S. Department of Energy (DOE) at the Atmospheric Radiation Measurement (ARM) site on Gan Island. The locations of the UM-Radiometer and DOE radiometer are shown in Figure 1. Furthermore, eight (8) radiosondes were launched daily from the DOE ARM site during DYNAMO, and these in-situ data were

used to develop the retrieval technique for clear sky conditions.

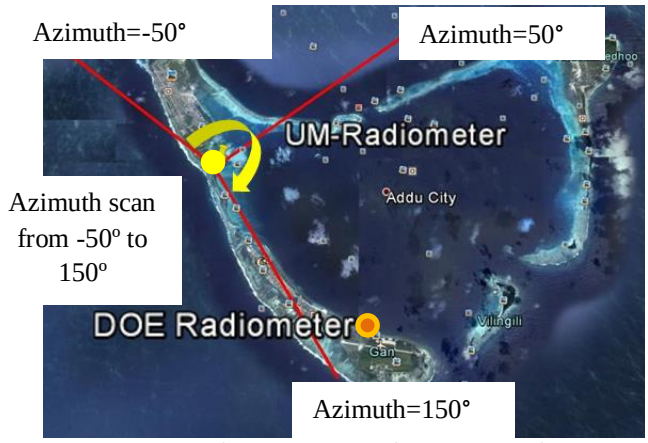

Figure 1. Map of the locations of University of Miami microwave radiometer (shown by the yellow disk) as well as DOE radiometer (shown by the orange disk) on Gan Island, The Maldives. The azimuth angle scan range for the UM-Radiometer is shown from -50° to 150°.

The radar was deployed to monitor clouds and to measure intensity and types of precipitation. It performed 360º azimuth scans at various elevation angles, including 5º, 7º, 9º, and 11º. The UM-Radiometer was deployed to measure water vapor and cloud liquid water. It sampled the atmosphere over the azimuth angle range of -50º to 150º at the elevation angles 5º, 7º, 9º, and 11º. The UM-Radiometer scanning pattern is shown in Figure 2 by the vertical solid blue lines and the horizontal dotted blue lines. The UM-radiometer's antenna beamwidth is 3.0º for 23.8 GHz channel and 3.3º for 30.0 GHz channel.

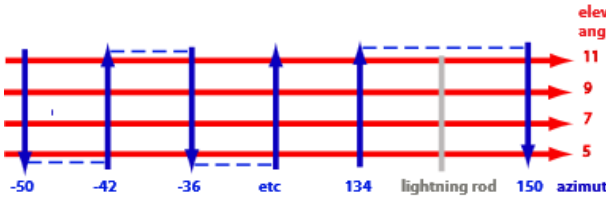

Figure 2. Radiometer scanning at various azimuth and elevation angles **[3]**.

3. DATA QUALITY CONTROL AND ANALYSIS OF MEASURED BRIGHTNESS TEMPERATURES

Brightness temperatures collected by the UM-Radiometer at the elevation angles of 5º, 7º, 9º, and 11º have been analyzed with respect to azimuth angle to detect any anomalous characteristics or land contamination. Measurements at various elevation angles were analyzed. The measured brightness temperatures at the frequencies 23.8 and 30.0 GHz and 5° elevation angle are presented with respect to azimuth angle in Figure 3 for the time period of 0 to 12 hours (UTC+5) on January 7, 2012. The fluctuations with respect to azimuth angle correspond to the varying atmospheric conditions (variation in water vapor) during the 12-hour period. Figure 3 shows an azimuth dependence of the mean brightness temperature, which is anomalous since the atmosphere should not show the same azimuth-dependent trend over a duration of 12 hours. Furthermore, this phenomenon has been observed in a number of datasets collected by UM-Radiometer during the DYNAMO campaign. This anomalous behavior of the measured brightness temperature needs to be analyzed.

Measurements at the azimuth angles -35º to 0º and 120º to 150º correspond to cases when the UM-Radiometer line of sight is over land, while the azimuth angle range 0º to 120º corresponds to the radiometer line of sight mostly over the ocean, as shown in Figure 1. Since the larger brightness temperature values correspond to line of sight over land, it is important to determine whether the anomaly is due to land contamination or variation in atmospheric conditions, including liquid water.

Various analyses have been performed to determine the nature of this anomaly. First, simulated brightness temperature from a radiosonde launched during the measurement are compared to the measured brightness temperatures at 23.8 and 30.0 GHz, shown by the blue and green circles in Figure 3, respectively. The simulated and measured brightness temperatures compare well only at azimuth angles near 50°. This analysis was not conclusive because it assumed that the atmosphere is homogeneous in azimuth angle, and there is no information about any possible azimuthal dependence, so this method will never be able to detect any anomaly.

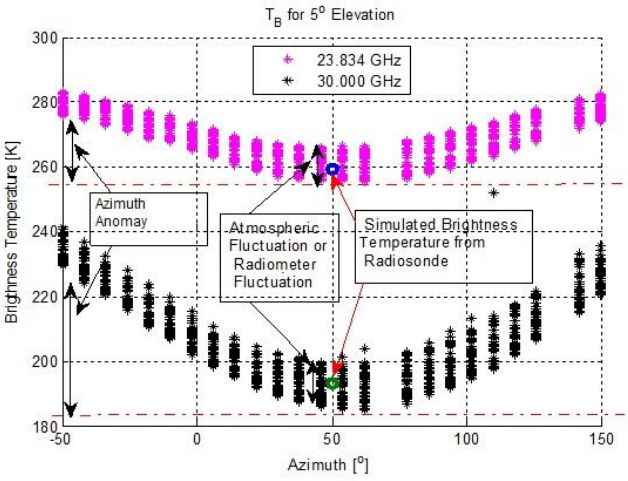

Figure 3. Measured brightness temperatures with respect to azimuth angle for 12 hours on January 7, 2012.

Next, scatter plots of measured brightness temperatures at 23.8 and 30.0 GHz during clear sky conditions at various azimuth angles are compared with those of simulated brightness temperatures at the same frequencies (from temporally collocated

radiosonde data) to compare the spectral signatures of simulated and measured brightness temperatures. Measured brightness temperatures from the dataset taken during the month of October 2011 are used for the analysis. Scatter plots for elevation angles 5° (top) and 7° (bottom) are shown in Figure 4. The radiometer-measured and radiosonde-simulated data compare well except a few cases for 7°elevation angle. If the measured brightness temperatures have contributions in addition to atmospheric variability, it will become evident in this analysis. Since this comparison shows that the radiometer-measured and radiosonde-simulated brightness temperatures are very similar, the anomalous behavior of the measurements may not be due to land contamination but instead are likely due to liquid water in the atmosphere.

Another analysis is the variation in the differences in brightness temperatures measured at azimuth angles -50° (with anomaly) and 54° (no anomaly) for 5° elevation angle. This variation is analyzed for both 23.8 and 30.0 GHz at noon and midnight for the 3-month period from October 7, 2011 to January 15, 2012.

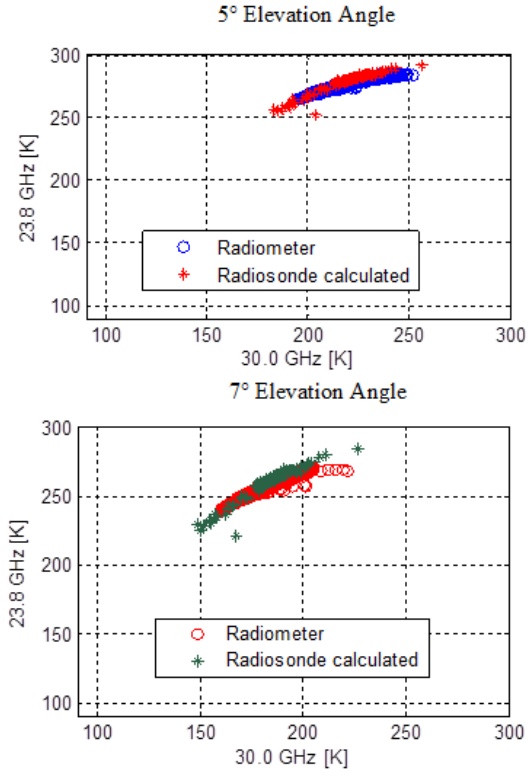

Figure 4. Scatter plots of 23.8 and 30.0 GHz brightness temperature measurements in comparison to simulations during clear sky conditions taken over a duration of 20 days of October 2011 during the DYNAMO experiment.

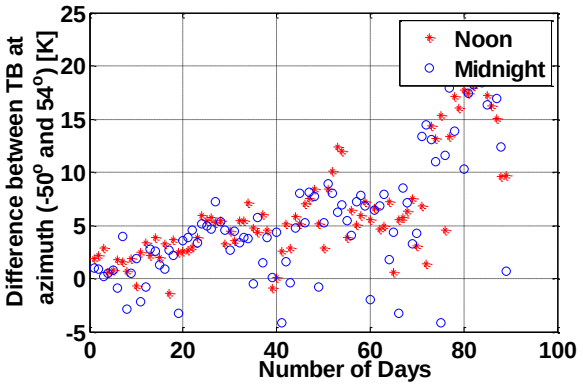

Figure 5. The difference of brightness temperature measured at -50° (with anomaly) and 54° (without anomaly) azimuth angles at 23.8 GHz at 5° elevation angle at noon and midnight for 90 days from October 7, 2011 to January 15, 2012.

Figure 5 shows the time evolution of these differences.

There is a generally increasing trend in brightness temperature difference at both noon and midnight. This trend is not affected by the time of day and is driven by change in atmospheric conditions over the 90-day period at both 23.8 and 30.0 GHz. If the brightness temperatures had been contaminated by land contributions, the difference during the day would be larger than the difference at night. This shows that the difference is not affected by land temperature. The same analysis has been performed for the brightness temperature differences at 30.0 GHz, the results of which are shown in Figure 6.

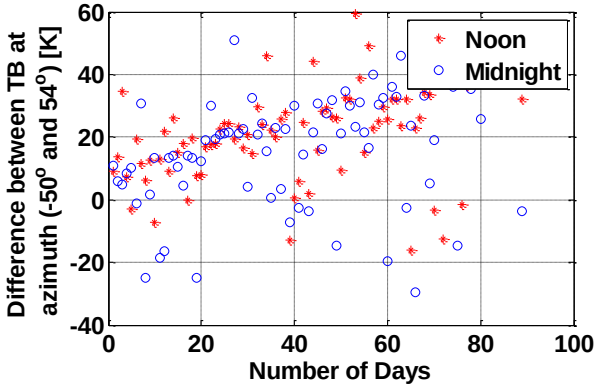

Figure 6. Same as Figure 5 except for 30.0 GHz instead of 23.8 GHz.

This difference also has a similarly increasing trend. However, the range of the differences at 30.0 GHz is approximately 4 times greater than at 23.8 GHz. As already mentioned, brightness temperatures at 30.0 GHz have significant contributions from liquid water and those at 23.8 GHz are mostly due to water vapor. From the above results and inferences, the source of the anomaly is likely to be liquid water instead of land contamination.

4. CLASSIFYING CLEAR SKY AND CLOUDY SKY CONDITIONS

As already discussed, one of the main objectives of this study is to develop a retrieval algorithm to estimate SWP from the UM-Radiometer at low elevation angles, i.e. 5º, 7º, 9º, and 11º. The retrieval has been developed based on linear regression analysis for measurements from only clear sky conditions. This restriction helps to simplify the analysis because of the impact of the low elevation angle on the retrieval. In the future, for a more advanced retrieval algorithm, both clear sky and liquid water will be considered.

The clear sky measurements need to be classified and then regressed with SWP from radiosonde data to determine the retrieval coefficients. As already mentioned, the 23.8 GHz and the 30.0 GHz brightness temperatures have major contributions from water vapor and liquid water, respectively. Taking this into consideration, during cloudy conditions or during rain, brightness temperatures at 23.8 and 30.0 GHz will be similar, while during clear sky conditions the brightness temperatures at 23.8 GHz will be much larger than that of 30.0 GHz. To distinguish the clear sky from cloudy conditions (integrated liquid water >> 0.03 mm), a cloudy sky ratio (CSR) was created, as Equation 1. This method is similar to that implemented by Bosisio et al. [4]. Intuitively, during clear sky conditions the CSR value will be larger than unity, while during rainy and cloudy conditions, the CSR value will be close to unity.

$$\mathrm{CSR}=\frac{TB_{23.8}}{TB_{30.0}} \qquad (1)$$

To demonstrate the CSR, brightness temperatures were simulated for 23.8 and 30.0 GHz using radiosonde data during clear sky conditions. Calculated CSR values for simulated brightness temperatures are shown in Figure 7. As shown in the figure, the CSR values for elevation angles of 5º, 7º, 9º, and 11º are approximately 1.25, 1.45, 1.55 and 1.65, respectively.

Based on this analysis, measurements performed by the UM-Radiometer during the DYNAMO experiment were used to calculate the CSR values, which in turn are used to distinguish clear sky and cloudy conditions. Here, the CSR values were calculated for the azimuth angles of -42° and 78° for the time period of 0 to 12 (UTC+5) for November 12, 2011. Figure 8 shows the CSR values for the azimuth angles of -42° and 78°.

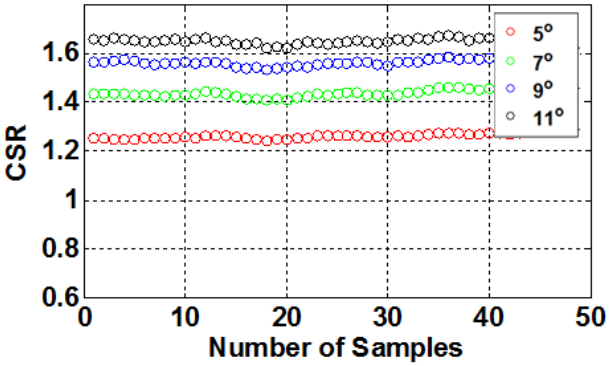

Figure 7. Cloudy sky ratio (CSR) values from simulated brightness temperatures for clear sky conditions.

The CSR values at both -42° and 78° azimuth angles are greater than unity at 0:00, as shown in Figure 7. At approximately 3:00 and 4:00, the CSR values at both azimuth angles are close to unity. For the azimuth angle of -42° the CSR values start increasing after 5:20, but for the azimuth angle of 78° the CSR values start increasing after 6:30. These CSR values for both azimuth angles are qualitatively compared with the reflectivity data measured by the S-PolKa radar for the presence of liquid water at the same azimuths as those shown in Figure 8.

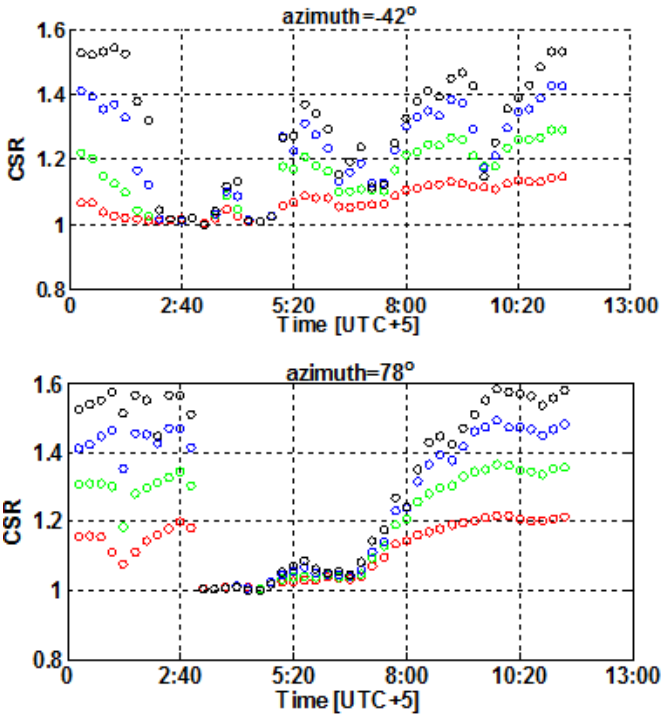

Figure 8. CSR values for November 12, 2011, from 0:00 to 12:00 (UTC+5) for the measurements taken at azimuth angle of -42° (top) and 78° (bottom).

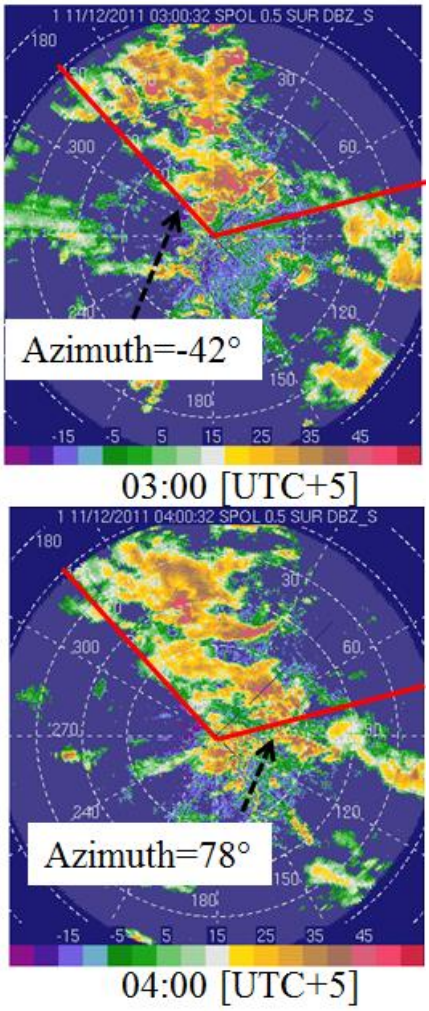

Figure 9. S-Pol radar reflectivity measurements showing the reflectivity values at 3:00 and 4:00 on November 12, 2011.

Figure 9 shows the radar reflectivity [5] data at 3:00 (UTC+5, upper panel) and 4:00 (UTC+5, lower panel) on November 12, 2011 for azimuth angles of -180 to 180º at a 0.5º elevation angle. The red segments show the azimuth angles of -42° and 78°. The reduced CSR values at 3:00 and 4:00 at the azimuth angles of -42° and 78° in Figure 8 are related to the amount of precipitation corresponding to the given radar reflectivity. The CSR values at 11:40 in Figure 8 correspond to the radar reflectivity values in Figure 10 when there is no reflectivity above the S-PolKa threshold, meaning no rain in this case. Therefore, for these times, the CSR values shown in Figure 8 show qualitative consistency with the S-Pol radar measurements shown in Figures 9 and 10.

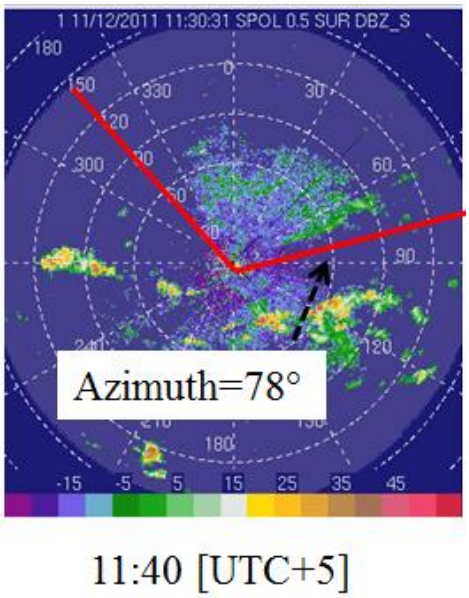

Figure 10. S-Pol radar reflectivity measurements showing the reflectivity values at 11:40 on November 12, 2011.

5. SUMMARY AND FUTURE WORK

This study demonstrates that the anomalous azimuthal behavior of 23.8 GHz and 30.0 GHz brightness temperature measurements measured at elevation angles of 5º, 7º, 9º, and 11º is most likely due to liquid water in the atmosphere. Measured brightness temperatures are classified into clear sky and cloudy sky conditions using the cloudy sky ratio method. Qualitative comparison with S-PolKa radar measurements at S-band show high consistency with the cloudy sky classifier.

Future work will focus on the development of a retrieval algorithm to retrieve slant water path during clear sky conditions. This algorithm will be improved to enable simultaneous retrieval of liquid water and SWP for cloudy sky cases. Retrieved slant water path in the presence of liquid water will be compared to the S-PolKa radar retrieved SWP [6] at various elevation and azimuth angles.

REFERENCES

[1] G. Farquharson, F. Pratte, M. Pipersky, D. Ferraro, A. Phinney, E. Loew, R. A. Rilling, S. M. Ellis and J. Vivekanandan, "NCAR S-Pol second frequency (Ka-band) radar," in *Proceedings of 32nd Conference on Radar Meteorology*, 2005.

[2] E. R. Westwater, "Ground-based microwave remote sensing of meteorological variables," in *Atmospheric Remote Sensing by Microwave Radiometry*, New York, Wiley, 1993, p. 145–214.

[3] P. Zuidema, "DYNAMO role of University of Miami scanning radiometer," Internal Report, 2011.

[4] A. V. Bosisio, P. Ciotti, E. Fionda and A. Martellucci,

"Rainy Event Detection by Means of Observed Brightness Temperature Ratio," in *12th Specialist Meeting on Microwave Radiometry and Remote Sensing of the Environment (Microrad)*, Rome, 5-9 March 2012.

[5] "DYNAMO Data Access," 2011. [Online]. Available: http://data.eol.ucar.edu/master_list/?project=DYNAMO. [Accessed 9 Sept. 2013].

[6] S. M. Ellis and J. Vivekanandan, "Water Vapor Estimates Using Simulataneous Dual-Wavelength Radar Observations," *Radio Sc.,* vol. 45, no. 5, p. DOI: 10.1029/2009RS004280, Oct. 2010.